

## A Simulation of Bomb Tritium Entry into the Atlantic Ocean

J. L. SARMIENTO

*Geophysical Fluid Dynamics Program, Princeton University, Princeton, NJ 08540*

(Manuscript received 22 September 1982, in final form 16 June 1983)

### ABSTRACT

Tritium is used in a model calibration study that is aimed at developing three-dimensional ocean circulation and mixing models for climate and geochemical simulations. The North Atlantic tritium distribution is modeled using a three-dimensional advective field predicted by a primitive equation ocean circulation model. The effect of wintertime convection is parameterized by homogenizing the tracer to the observed March mixed-layer depth. Mixing is parameterized by horizontal and vertical Fickian diffusivities of  $5 \times 10^{-6} \text{ cm}^2 \text{ s}^{-1}$  and  $0.5 \text{ cm}^2 \text{ s}^{-1}$ , respectively.

The spreading of tritium in the model is dominated by advection in the horizontal, and by wintertime convection and advection in the vertical. The horizontal and vertical mixing provided by the model have negligible effect. A comparison of the model tracer fields with observations shows that most of the basic patterns of the tritium field are reproduced. The model's mean vertical penetration of 543 m in 1972 is comparable to the 592 m penetration obtained from the data. The major discrepancy between model and data is an inadequate penetration into deeper portions of the northwestern subtropical gyre main thermocline. Some of the problems that may contribute to this are identified.

A tritium simulation with a smoothed input gives a penetration depth of only 395 m. The smoothing puts a high fraction of the tritium into low-latitude, low-penetration regions such as the equator. This suggests that great care needs to be exercised in using simplified models of tritium observations to predict the behavior of tracers with different input functions, like fossil fuel  $\text{CO}_2$ .

### 1. Introduction

An ultimate goal of any effort to predict the role of the oceans in climate change and in determining the fate of anthropogenic substances must be the development of accurate models of global ocean circulation and mixing. The need to predict the climate changes that are expected to accompany the addition of fossil fuel  $\text{CO}_2$  to the atmosphere gives added urgency to the efforts to develop such models. The oceans are the primary sink for fossil fuel  $\text{CO}_2$ , and so figure centrally in any attempt to predict future levels of  $\text{CO}_2$  in the atmosphere. Also, it is expected that the enormous heat capacity of the oceans will have a significant impact on the rate at which the earth's climate responds to the  $\text{CO}_2$  transient.

Some of the most powerful tools for the verification and tuning of models of the climatic-time-scale oceanic circulation and mixing are chemical tracers. Salinity, oxygen, the nutrients and radiocarbon have been used along with temperature for verification in a great variety of model studies. Noteworthy examples of three-dimensional tracer studies are Arons and Stommel (1967), Kuo and Veronis (1970, 1973), Fiadeiro and Craig (1978), and Fiadeiro (1982), all of which use a circulation pattern determined by Stommel's (1958) approach. Holland (1971) used a "primitive" equation ocean general circulation model

of the type introduced by Bryan (1969). The Holland study along with the others have clearly demonstrated the value of chemical tracers for model verification.

Tritium is a relatively new chemical tracer which is important because its time scale and the regions of the oceans where its impact is felt are those of most interest to us in understanding the fossil fuel  $\text{CO}_2$  problem and the earth's climate. Tritium was produced by the nuclear bomb tests of the late 1950's and early 1960's in an amount greatly exceeding its natural abundance. Its input to the surface oceans as water (HTO) has been reconstructed using a hydrologic model and measurements of tritium in rain (Weiss *et al.*, 1979; Weiss and Roether, 1980). There are a large number of oceanic measurements of this tracer, particularly in the Atlantic Ocean between 1971 and 1974 (Östlund *et al.*, 1974a, 1976, 1977; Roether and Weiss, 1978; and unpublished results of W. Roether, University of Heidelberg). The Transient Tracers in the Oceans Project has recently completed a new data set in the same area and will gradually cover the rest of the world ocean.

The distribution of tritium in the North Atlantic has been studied by several investigators using descriptive as well as modeling approaches (Münnich and Roether, 1967; Östlund *et al.*, 1969; Rooth and Östlund, 1972; Östlund *et al.*, 1974b; Roether and Weiss, 1978; Broecker and Östlund, 1979; Jenkins,

1980; Sarmiento *et al.*, 1982a; Sarmiento, 1983). This paper documents the first effort to develop techniques for the verification of a three-dimensional primitive equation ocean circulation model with tritium as a tracer. The model is used, in turn, to gain some insight into the mechanisms leading to the observed tritium distribution. The greater amount of tritium data available in the North Atlantic motivated the decision to set the model in the Atlantic from 20°S to 67°N.

The advective field used in the present study is obtained from the "free thermocline" model of Sarmiento and Bryan (1982). This model restores the predicted temperature and salinity fields toward the observed fields with a damping term in the surface layer and below 1000 m. In the surface layer the restoring term serves as the boundary condition for heat and salt. The restoring term is retained below 1000 m in order to speed up convergence to a solution.

The equilibrium advective field predicted by the free thermocline model is used in a separate simulation in which only the tracer conservation equation is solved. Convective processes are included by a simplified parameterization of wintertime convection as described below.

The basic procedure followed is to predict the tritium distribution starting in 1952 and ending at the end of 1972 using the Weiss *et al.* (1979) input function. The model results are then compared with oceanic measurements for the period 1971–74 as analyzed for the end of 1972 by the objective analysis method described by Sarmiento *et al.* (1982b).

The 10-year period between the production of most of the tritium by the thermonuclear bomb tests of 1962 and the 1972 observations is short enough that ~90% of the tritium is still in the main thermocline. The discussion of the results thus focuses entirely on the upper part of the water column.

The tritium simulation points to a number of shortcomings in the ocean circulation model, many of which can be remedied quite easily. Further work is now proceeding to make the predictions more quantitatively correct. Despite the limitations of the ocean circulation model, many important things have been learned from this study about the mechanisms giving rise to the observed tritium distribution. It also serves as an illustration of techniques that can be used to calibrate ocean circulation models with tritium observations.

The paper begins with a description of the tritium model. This is followed by an analysis of the tritium simulation based on a comparison with data.

## 2. The tritium model

The equation solved in the tritium simulation is the equation of conservation

$$\frac{\partial T}{\partial t} + \mathbf{v} \cdot \nabla T + w \frac{\partial T}{\partial z} = A_{TH} \nabla^2 T + \frac{\partial}{\partial z} \left( A_{TV} \frac{\partial T}{\partial z} \right) - \lambda T + \text{sources}, \quad (1)$$

where  $\mathbf{v}$  and  $w$  are the horizontal velocity vector and vertical velocity, respectively, obtained from the ocean circulation model, and  $\lambda$  is the decay constant for tritium,  $1.79 \times 10^{-9} \text{ s}^{-1}$  (the mean life is 17.7 years)<sup>1</sup>. The effect of sub-grid-scale motions on the larger scale fields is parameterized by Fickian diffusion with horizontal mixing  $A_{TH}$ , and vertical mixing  $A_{TV}$ , set equal to  $5 \times 10^6 \text{ cm}^2 \text{ s}^{-1}$  and  $0.5 \text{ cm}^2 \text{ s}^{-1}$ , respectively. The source term is the input of tritium at the ocean surface. The tritium concentration  $T$  is in tritium units, the number of tritium atoms per  $10^{18}$  hydrogen atoms.

A major problem with the first simulations that were done was the failure of tritium to penetrate downward as rapidly as the observations indicate it should. A proper simulation of the overall penetration is extremely important for obtaining realistic tracer and heat distributions. The primary reason for this problem was that the tracer model had no convection. The effect of wintertime convection was thus included in as simple a fashion as possible by imposing convection to the depth of the March mixed layer [Fig. 1, taken from Levitus (1982)]. This is the month of the maximum mixed-layer penetration. The convection is done by vertically homogenizing the tracer concentration over the depth range shown in Fig. 1 during each time step while conserving mass.

The finite difference scheme used is second order in time and space and includes some of the energy conserving constraints of Arakawa (1966) as explained by Bryan (1969). The algorithm is that of Bryan (1969) and Semtner and Mintz (1977) modified for the Geophysical Fluid Dynamics Laboratory computer.

The model covers the same region of the Atlantic Ocean as that of Sarmiento and Bryan (1982): 20°S to 67°N. The northern boundary coincides with the ridge separating the Norwegian and Greenland Seas from the open Atlantic. The southern boundary was chosen well south of the equator so that the equatorial region could be simulated with less distortion.

The equation is solved at 12 levels in the vertical that are arranged to allow for maximum resolution in the upper thermocline (see Table 1).

The boundary conditions are no flux of tracer across the ocean floor and all sidewalls. The flux at

<sup>1</sup> After this study was completed it was learned that an improved estimate for the decay constant of tritium is  $1.77 \times 10^{-9} \text{ s}^{-1}$  (Mann *et al.*, 1982). This change would have a negligible effect on the results.

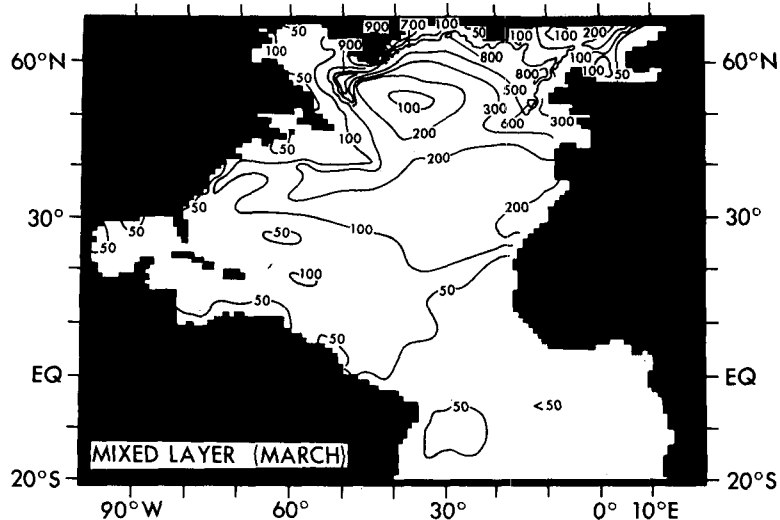


FIG. 1. The thickness of the mixed layer in March calculated in meters from climatic mean potential temperature data mapped by Levitus (1982).

the surface is specified as a function of space and time using the input function reconstructed by Weiss *et al.*, (1979). The Weiss *et al.* input function is based on observations of tritium concentration in rainfall and a hydrologic model which includes water vapor exchange. The tritium concentrations in rainfall are taken by Weiss *et al.* to be representative of the water vapor tritium concentrations. They discuss evidence which supports this assumption.

There are three basic components to the Weiss *et al.* input function. The first is the input from air masses that reside primarily over the sea. This input is dependent on latitude and rainfall, and is dominated by gas exchange. The oceanic tritium concentrations used in calculating back flux by gas exchange are those calculated by the model.

The second component is the input from air masses that move out over the sea from the land. Weiss *et al.* show that these air masses have higher inputs for a given latitude than do marine air masses, because gas exchange over land is not as effective in removing tritium as it is over the ocean. This gives rise to tritium concentrations in continental air about four times higher than those in marine air. The distance over which this input is effective has an *e*-folding length of  $\sim 300$  km from the land.

The third component is river input. For the case to be described here the riverine tritium input is all placed in the western Atlantic at the surface grid point nearest the continental margin. The actual eastern Atlantic input is a negligible part of the total and it is simpler to put this input in the western Atlantic.

The input function of Weiss *et al.* goes only to the equator. The input they give for the equator is used

from  $0^\circ$  to  $20^\circ\text{S}$  except that the riverine and continental air inputs are omitted.

The total tritium in the model ocean is shown as a function of time in Fig. 2. The majority of the tritium enters the oceans between 1962 and 1964 after which time the tritium slowly decreases, due primarily to decay. The total tritium predicted for 1972 using Weiss's input is 612 MCi, which is considerably larger than an estimate of 512 MCi based on the oceanic observations described by Sarmiento *et al.* (1982b). The difference of 16% is not unreasonable, given the assumptions that Weiss *et al.* must make in constructing their input function. It does make it difficult to directly compare maps produced from the data with maps produced by the model. Since the tracer conservation equation is linear, one can correct the model results by reducing concentrations at all lo-

TABLE 1. Depths of levels in the model.

| Level | Depth (m) |
|-------|-----------|
| 1     | 25        |
| 2     | 81        |
| 3     | 159       |
| 4     | 274       |
| 5     | 451       |
| 6     | 713       |
| 7     | 1087      |
| 8     | 1588      |
| 9     | 2216      |
| 10    | 2955      |
| 11    | 3782      |
| 12    | 4671      |

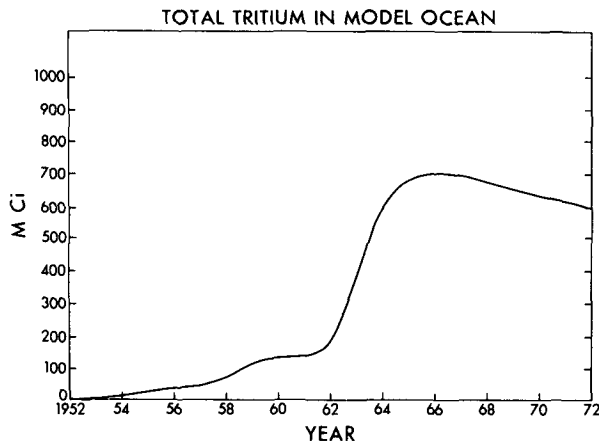


FIG. 2. Integrated tritium in the model as a function of time.

calculations by 16%. All the model plots shown below have this correction.

### 3. Results

The first subsection reviews briefly the major features of the ocean circulation model in order to provide a setting for the discussion that follows. Most of the 1971–74 tritium data is along the north–south west Atlantic GEOSECS section (Östlund *et al.*, 1976) and the two east–west NAGS sections at 14°N and 29°N (Östlund *et al.*, 1977). The second subsection thus discusses the comparison between model and data along these three vertical sections. A third subsection discusses the comparison between horizontal maps of model results and the maps produced from 1971–74 data by Sarmiento *et al.* (1982b). The final two sections discuss various analyses of the horizontal redistribution and vertical penetration of tritium in the model.

#### a. Ocean circulation

Fig. 3 shows horizontal trajectories spanning a full year at three levels of the free thermocline model of Sarmiento and Bryan (1982). The dots indicate the terminus of the trajectory. Fig. 4 shows the zonally integrated meridional overturning in the model. The contour interval is 5 Sverdrups ( $1 \text{ Sv} = 10^6 \text{ m}^3 \text{ s}^{-1}$ ).

The trajectories at 25 m are dominated by the wind-driven Ekman transport. There is a relatively shallow upwelling of the order of 15 Sv in the equatorial region (Fig. 4) with poleward transport at the surface in both hemispheres (Fig. 3a). The surface poleward transport in the Northern Hemisphere is of the order of 10 Sv. This poleward transport ends just south of 30°N. North of that, the Ekman transport is toward the south. North of ~50°N the transport again changes direction as one leaves the subtropical gyre and enters the subpolar gyre. Within most of the subtropical gyre, the wind-

driven transport is convergent and thus gives rise to downwelling (Fig. 4). The subpolar gyre is characterized by upwelling which is very shallow and small in total volume.

The trajectories at 159 and 451 m are very similar to those that would be expected from geostrophic calculations. The dominant features are the Gulf Stream, its extension as the North Atlantic current, and the subtropical gyre. The southern boundary of the subtropical gyre is in the north equatorial current at ~15°N on the 159 m surface. The boundary moves to just south of 30°N on the deeper surface. A complete circuit around the gyre at either level takes of the order of 10 years except near the North American coast where the trajectories show a nearly closed loop in approximately one year.

The large-scale thermohaline overturning is shown in Fig. 4. Deep water formation in the North Atlantic is of the order of 15 Sv. Approximately 10 Sv recirculate mostly north of the equator. Another ~5 Sv go to the southern boundary where they upwell into the thermocline. Sarmiento and Bryan (1982) discuss the boundary conditions at this wall. The 5 Sv then move to the north at an intermediate depth, upwell at the equator, downwell at ~25°N, and join the ~10 Sv of thermohaline circulation which recirculates north of the equator. North of ~30°N there is a large northward transport concentrated within the main thermocline which feeds the thermohaline circulation and the subpolar gyre upwelling (Fig. 3). This circulation pattern has a strong impact on the tritium distribution, as will be discussed below.

#### b. Vertical sections

The model sections are from the last time step in 1972. The data used are raw measurements with a small correction for decay to the end of 1972. Fig. 5 shows the tritium distribution in the top 1000 m along the west Atlantic GEOSECS track. The model reproduces most of the major features observed in the data such as the low tritium penetration in the equatorial region which is a result of upwelling of low tritium Southern Hemisphere water, the strong horizontal gradient region or “front” at about 15°N near the surface which shifts toward higher latitudes with increasing depth, and the intermediate maximum at about 100–200 m found between about 10 and 30°N. The model also has high near-surface concentrations at ~50°N in the same region as the data. This is water coming out of the Labrador Sea.

The intermediate maximum between 100 and 200 m arises from the generally southward transport of tritium-rich waters in the subtropical gyre below the surface [Subtropical Underwater (Defant, 1936); see Fig. 3b] overlain by northward moving equatorial tritium poor waters [Fig. 3a (see discussion by Sarmiento *et al.*, 1982)].

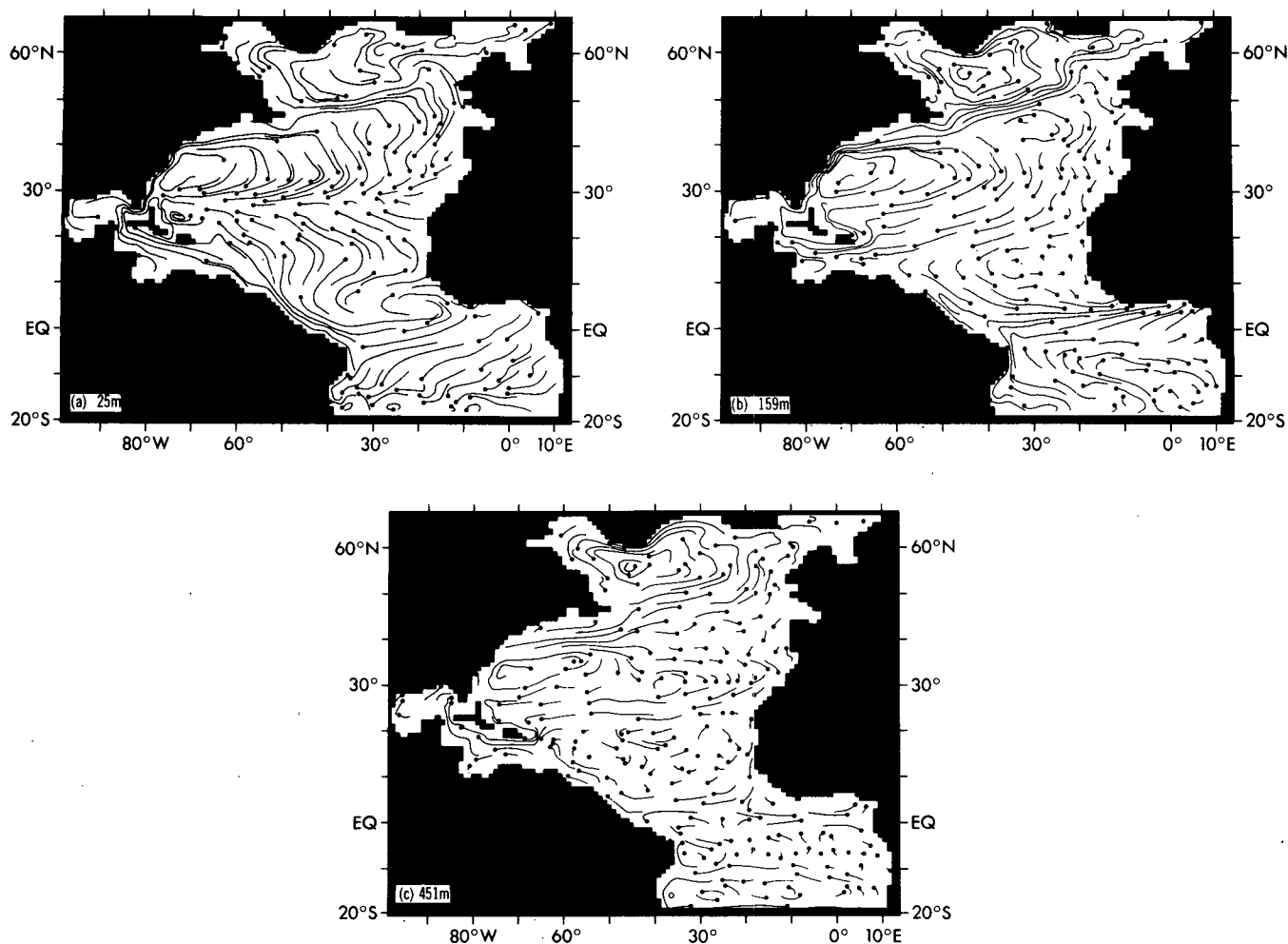


FIG. 3. Trajectories of one year's duration calculated with velocities taken from the free thermocline model of Sarmiento and Bryan (1982). The point marks the end of the trajectory. (a) Level 1 of the model at 25 m, (b) level 3 at 159 m, (c) level 5 at 451 m.

The front at  $\sim 15^\circ\text{N}$  is maintained by several processes. The circulation here is primarily zonal (the North Equatorial Current) with very little meridional advective exchange (Fig. 3). North of the front the Subtropical Underwater carries tritium rich water to the south, but much of this upwells (Fig. 4). In addition, there are  $\sim 5$  Sv of northward flow from the equator (Fig. 4) that are continually feeding in water which is tritium free. As will be seen below in discussing the horizontal redistribution of the tracer, the meridional circulation is the dominant tracer transport process in this region at all times, and it is always to the north.

One of the main failures of the simulation along this section is the insufficient vertical penetration of tritium between about  $20$  and  $50^\circ\text{N}$ . South of  $\sim 20^\circ\text{N}$  the penetration is somewhat too deep. The intermediate maximum between  $10$  and  $30^\circ\text{N}$  is also somewhat deep and rather sharp, a consequence

mainly of overly strong southward advection at the depth of the maximum. The latter results from the deepening of the thermocline in the free thermocline

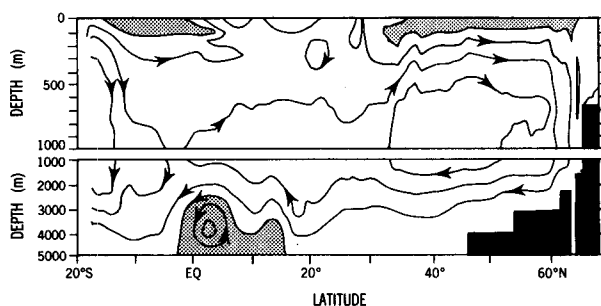


FIG. 4. Zonally integrated meridional transport in the free thermocline model of Sarmiento and Bryan (1982). Contour interval is 5 Sv. Negative values are shaded.

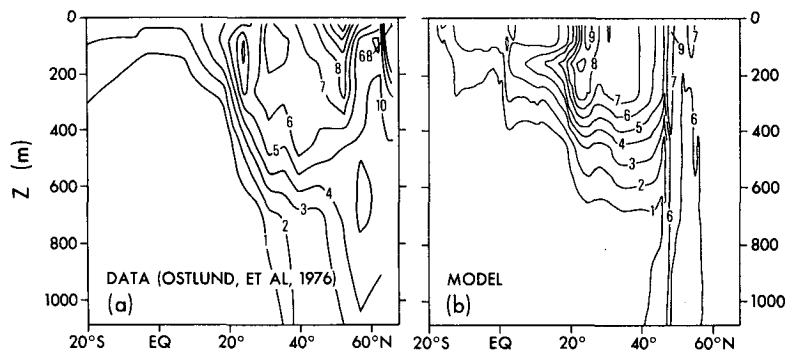


FIG. 5. Tritium on the north-south GEOSECS section in the western Atlantic. (a) Measurements made in 1972 (Östlund *et al.*, 1976), (b) model prediction.

model that was noted by Sarmiento and Bryan (1982). Their robust diagnostic ocean circulation model, which adheres more closely to the observed density field than the free thermocline model used here, has a more zonal flow in this region. A tritium simulation that was done with the robust diagnostic model gives a much better simulation of the intermediate maximum.

The free thermocline tritium simulation gives an unrealistic minimum in tritium concentration in deeper waters at  $\sim 50^\circ\text{N}$  (Fig. 5). This minimum is advected in by the Gulf Stream extension from the North American continental margin where it is generated by upwelling, as will be discussed below.

Fig. 6 shows the tritium distribution in the upper 1000 m on a section at  $29^\circ\text{N}$  that was measured as part of the North Atlantic Gyre Study (Östlund *et al.*, 1977). This section illustrates the point made earlier about insufficient vertical downward penetration north of  $20^\circ\text{N}$ . There is a downward slope toward the west in the model concentration isopleths. This is due primarily to the deeper penetration of tracer in the western Atlantic that occurs by the downward

spiraling of tracer trajectories in the recirculation region (Cox, 1983).

Fig. 7 shows the tritium distribution along the  $14^\circ\text{N}$  NAGS section. The intermediate maximum and downward slope of the isopleths toward the west is reproduced satisfactorily. As explained above, the intermediate maximum is associated with the Subtropical Underwater. The downward slope to the west of the isopleths develops because this section cuts across the geostrophic flow (North Equatorial Current) which trends approximately northeast to southwest (Fig. 3b). The northern portion of the current carries high tritium subtropical waters whereas the southern portion carries low tritium equatorial waters. The tritium in the subsurface maximum is somewhat higher in the model than observed, because the surface concentrations to the north, where the Subtropical Underwater forms, are too high (Fig. 8).

### c. Horizontal maps

Fig. 8 shows horizontal maps of the tritium distribution at the end of 1972 at three depths equivalent to levels 1, 4 and 5 of the model. The model maps

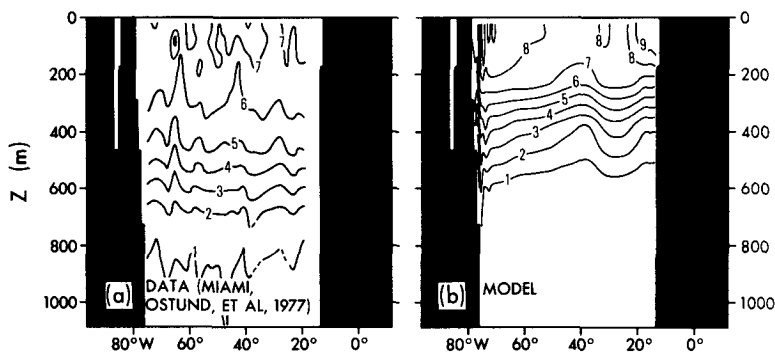


FIG. 6. Tritium on an east-west section at  $\sim 29^\circ\text{N}$  in the North Atlantic. (a) Measurements made in 1972 (Östlund *et al.*, 1977), (b) model prediction.

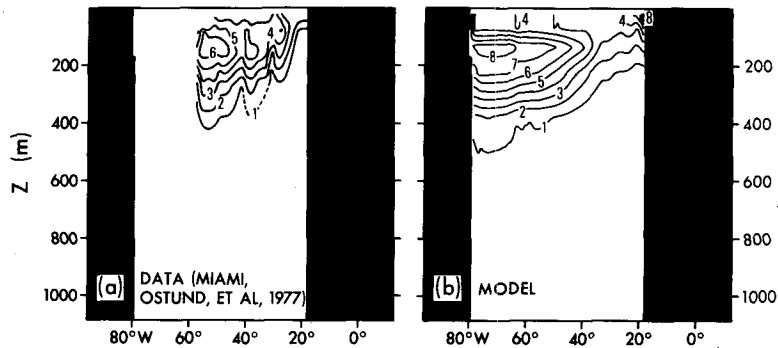


FIG. 7. As in Fig. 6 except at  $\sim 14^\circ\text{N}$ .

are from the last time step in 1972. Levels 2 and 3 are similar to level 4 so they are not shown here. The objective analysis technique used to produce the data maps smooths the measurements (see Sarmiento *et al.*, 1982b). The model simulation results have not been smoothed in order to preserve the details of the tracer field. In comparing the model results to the data maps, only the large-scale features of the field will be emphasized.

Levels 1–4 of the model are  $\sim 0.5$  TU too high on the average, whereas level 5 is almost one TU too low. This is because of inadequate vertical penetration. The low concentrations at level 5 are a major failure in the model simulation and will be discussed in more detail in Section 4.

The model has more small-scale features than the data at all levels, but most of these disappear with smoothing except for the high concentrations in the vicinity of  $30^\circ\text{N}$  at levels 1–4. This is the region of Ekman convergence in the model and it is this convergence which gives rise to the maximum. The existence of such a maximum is not supported by the data that have been used in preparing the maps in Fig. 13. The reason for this discrepancy between model and data is not clear at this time. It may be that the inclusion of seasonal forcing in the model, which would continually shift the pattern of Ekman convergence, would give rise to a tritium distribution more like that observed in the data. It is possible that the model parameterization of mixing contains important errors or that the input function is in error. Finally, it is possible, though less likely, that there are simply too few stations to represent the maximum in the data maps.

Another feature not supported by the data, that remains even after smoothing, is the southward penetration of tracer across the North Equatorial Current in the western Atlantic at level 4. This is due to the southward transport that results from the deepening of the thermocline as discussed in connection with the GEOSECS section above.

Despite the problems mentioned above, most the

major features of the tritium distribution, such as the front at  $\sim 15^\circ\text{N}$  and the fairly smooth tritium concentrations within the subtropical gyre, are simulated quite successfully. The free thermocline ocean circulation model is able to reproduce the rapid recirculation within the gyre, and the slow exchange across the southern boundary of it, that give rise to the front and smoothing within the gyre. Sarmiento *et al.* (1982a) have discussed these processes in more detail.

An important feature of the horizontal distributions that will have bearing on the discussion below of horizontal transport of tracer is that the northward moving portion of the gyres shown in Fig. 3 have lower concentrations than the southward moving portion at almost all levels. This gives rise to a net southward tracer transport due to the gyre component of the total transport that will be discussed below. The low tritium concentrations in the model near the North American continent are associated with upwelling there. The Gulf Stream and North American current carry these low tritium waters to the north and east. There are no data near North America that can be used to show whether or not such a feature exists in nature. However, it is probable that the shallow southward transport of tritium-rich water from the Labrador Sea along the North American continent, which has been observed but is not reproduced in the model (Sarmiento and Bryan, 1982), contributes toward increasing the tritium along the continental margin. This is definitely an area where further work needs to be done with modeling and, more importantly, with observational studies.

#### d. Horizontal redistribution

One can form an impression of the horizontal redistribution of tracer from a comparison of the 1972 tritium standing crops (vertical integral of the tritium concentration) of the model (Fig. 9b) with the integrated decay corrected input (Fig. 9a), and from a plot of the northward tracer flux for various times (Fig. 10). We now let brackets denote a zonal average, i.e.,

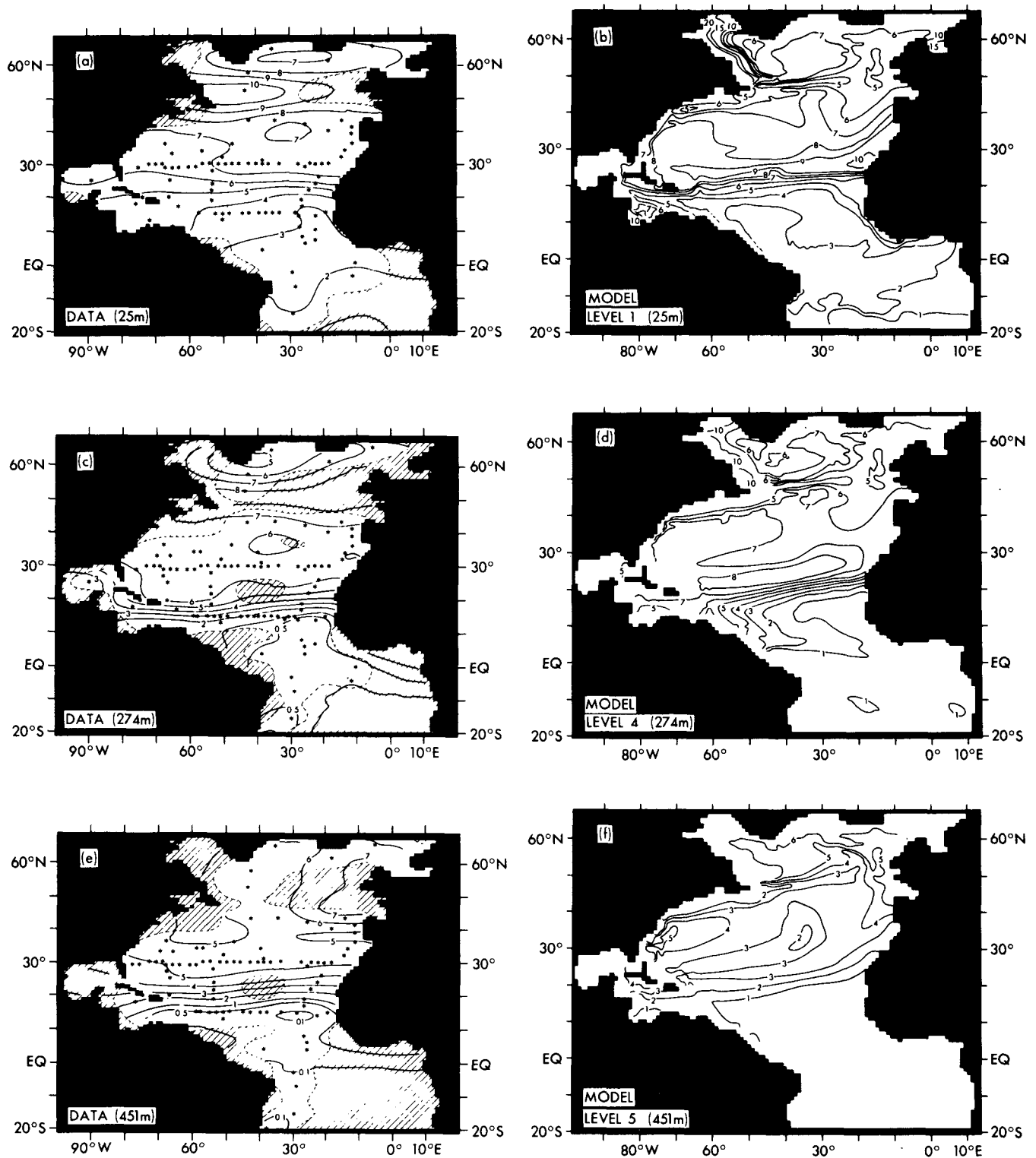


FIG. 8. Horizontal maps of tritium at the end of 1972 at various depths. The data are mapped as described by Sarmiento *et al.* (1982b). (a) and (b), Data and model, respectively, at level 1 (25 m); (c) and (d), data and model at level 4 (274 m); (e) and (f), data and model at level 5 (450 m).



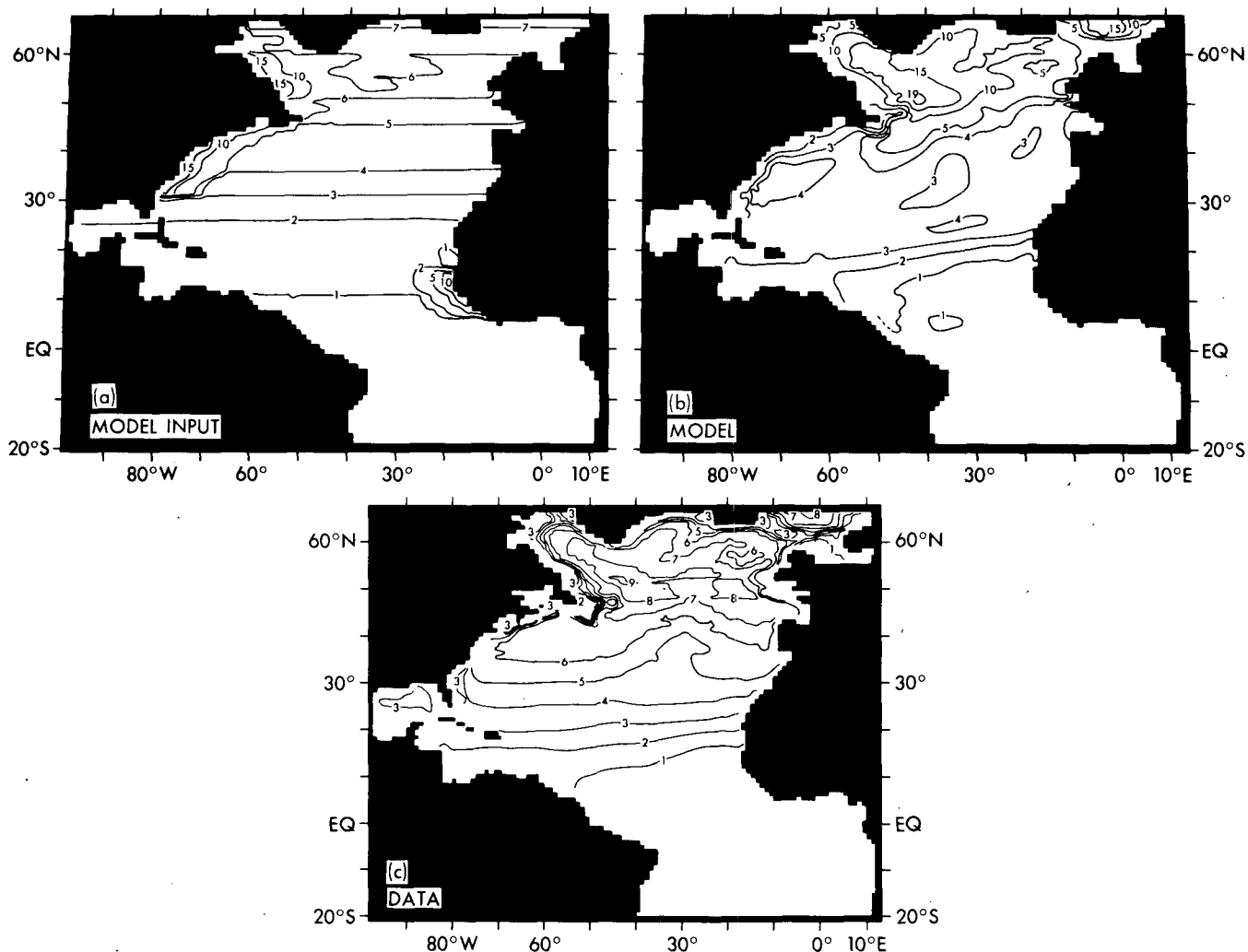


FIG. 9. The standing crop of tritium ( $\int T dz$ ) in KTU-m at the end of 1972, using (a) the decay corrected input adapted from Weiss *et al.* (1979). Not shown is the river input in the  $1^\circ$  squares nearest the land on the western margin of the ocean. The total river input is just over 10% of the total input from all sources. The only regions where the river input makes a substantial contribution of  $>10\%$  of the zonal total is in the Labrador Sea and on the Equator in the vicinity of the Amazon, where the river input is about one-third the zonal total. (b) The model prediction. (c) Observations mapped by the technique of Sarmiento *et al.* (1982b).

$$[\ ] = \frac{\int ( ) a \cos \phi d\lambda}{\int a \cos \phi d\lambda}, \quad (2)$$

where  $a$  is  $r_e/180$ ,  $r_e$  is the radius of the earth,  $\phi$  latitude, and  $\lambda$  longitude. The northward tracer flux is then

$$F = \iint [vT] a \cos \phi d\lambda dz. \quad (3)$$

Fig. 9 shows that there is a loss in the model of tracer from the equatorial zone, particularly between  $\sim 5$  and  $15^\circ$ N. This has been documented for the case of carbon-14 from observations (Broecker *et al.*, 1978) and is related to the equatorial upwelling and

poleward wind-driven surface advection. One can see in Fig. 10 that the tracer removal in the model is mainly due to a northward transport of tracer in the Northern Hemisphere which is particularly strong in the years near the time of peak input in 1963–64. The region of northward transport continues to  $\sim 23^\circ$ N. The tracer that is being removed from the equatorial zone is deposited between  $\sim 15$  and  $23^\circ$ N. The overall trend of the transport in this region is northward through most of the period of the simulation until 1972. However, the magnitude of the transport decreases with time.

Between  $\sim 23$  and  $40^\circ$ N is a region of southward tracer transport (Fig. 10), with loss occurring between  $\sim 30$  and  $40^\circ$ N, and accumulation occurring between

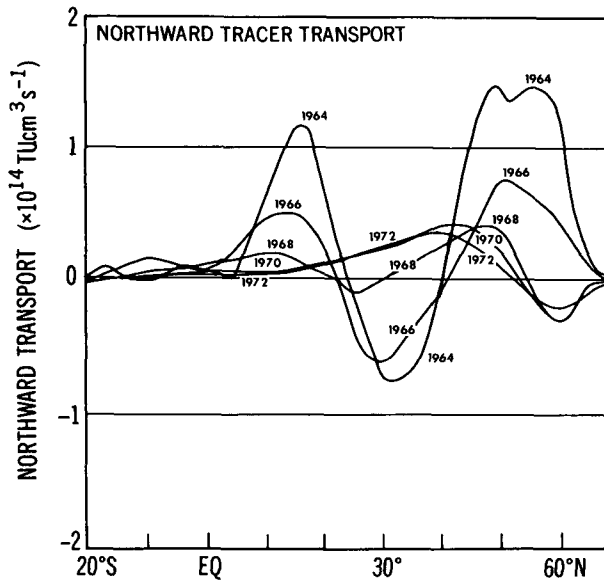


FIG. 10. Northward tracer transport for various years for the model calculated from Eq. (3).

~23 and ~30°N. Here, too, the tracer transport decreases with time. The transport changes sign by 1970 and is to the north after this, like the heat flux in this area (Sarmiento and Bryan, 1982).

North of ~40°N, the transport is northward in early years, decreasing, and finally becoming southward in part of the region in later years. There is a considerable accumulation of tracer north of ~55°N, primarily to the east of Iceland (Fig. 9).

Thus the overall effect of the transport illustrated in Fig. 10 is to accumulate tracer in the region between ~15 and 30°N as well as north of ~55°N, while removing it from south of ~15°N and from the area between ~30 and 55°N. This transport takes place mainly before ~1968.

A comparison of the model standing crops (Fig. 9b) with the data (Fig. 9c) shows that the model simulation is deficient in tritium in the region between ~25 and 50°N, and too high to the north of this. The basic problem with the model simulation thus appears to be that tritium is lost at too high a rate from the region between 25 and 50°N to the region north of 50°N. This is another major failure of the tritium model simulation that will be discussed in more detail later. The loss toward the south from north of 25°N does not appear to be excessive; the model standing crops south of 25°N are comparable to the data standing crops.

It is interesting to separate the northward tracer flux into components (Fig. 11) as has been done for heat flux (Sarmiento and Bryan, 1982). Using the definition in (2), we have the northward tracer flux given by

$$F = Z + G + D, \tag{4}$$

where

$$Z = \iint [V][T]a \cos\phi d\lambda dz, \tag{5}$$

$$G = \iint [V'T']a \cos\phi d\lambda dz, \tag{6}$$

$$D = \iint A_{HH} \frac{\partial [T]}{\partial \phi} a \cos\phi d\lambda dz. \tag{7}$$

Primes denote departures from zonal averages,  $Z$  is the tracer transport due to meridional overturning in the vertical plane,  $G$  (gyre) is the tracer transport due to correlations between  $V$  and tracer concentrations in the horizontal plane, and  $D$  (diffusion) is due to horizontal mixing. The gyre term is also referred to as the eddy component of the transport.

The tracer transport is dominated by the meridional and gyre components (Fig. 11). The diffusion component is negligible almost everywhere.

The meridional component is generally to the north, due to the northward flow of tritium-bearing waters in the upper part of the water column compensated by a return flow of tritium-free waters at depth. In the northern half of the subtropical gyre, the Ekman flow in the surface layer carries tritium to the south. However, convection rapidly removes

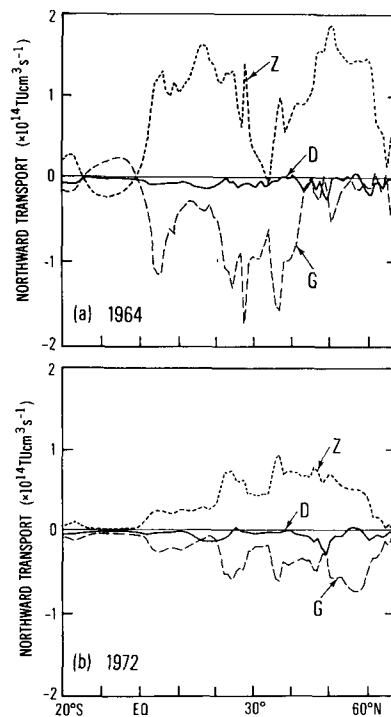


FIG. 11. Components of the northward tracer transport for the model calculated from Eqs. (5), (6) and (7) in the text for (a) the end of 1964, and (b) the end of 1972.

tritium from this layer into the northward moving waters below. It is interesting to contrast this model with one that has no convection. In the latter case, the northward meridional overturning is less in the northern half of the subtropical gyre because the tritium remains longer in the southward moving Ekman transport at the surface. The situation at  $\sim 35^\circ\text{N}$  is unusual in that it has a zero northward meridional overturning in 1964. Apparently, in 1964, the tracer has not yet penetrated to the region of northward transport below the surface.

The gyre component of the tracer flux is generally southward. There are three important gyre circulation boundaries which occur at  $\sim 15^\circ\text{N}$ , just south of  $\sim 30^\circ\text{N}$  on deeper surfaces, and at  $\sim 50^\circ\text{N}$  (Fig. 3). The southward tracer transport is at a minimum at these boundaries (Fig. 11). There is southward tracer transport within each of the gyres because the northward branch carries water with lower tritium than the southward branch (Fig. 8). Much of this gyre transport is quite shallow. A model that has no wintertime convection thus exhibits a greater southward transport in 1964 and has too much tritium south of  $\sim 25^\circ\text{N}$ .

The gyre and meridional components are opposite in sign almost everywhere. In 1972 there is almost complete cancelation between these components, except for a small positive remnant at lower latitudes, and a negative remnant north of  $\sim 50^\circ\text{N}$ .

A similar cancelation was first observed in a stratospheric tracer simulation by Hunt and Manabe (1968), and has been discussed by a variety of investigators (see review by Mahlman *et al.*, 1981). This "non-transport" occurs in the oceans after the tritium source becomes small. The tritium eventually achieves a quasi-stationary distribution in which it has essentially constant concentrations on isopycnal surfaces within the subtropical gyre (Sarmiento *et al.*, 1982). At this point there will be only a small amount of net transport taking place. However, the breakdown of transport along isopycnal surfaces into horizontal and vertical components can give quite large transport components which essentially cancel each other.

In the case of heat flux, such a cancelation does not occur. The meridional overturning is dominant over all other components throughout most of the model-ocean. This is because heat maintains strong sources and sinks at all times. An obvious suggestion, based on the foregoing, is that the tracer transport should be analyzed along isopycnal surfaces using a Lagrangian perspective (e.g., Mahlman *et al.*, 1980). This work has yet to be done.

#### e. Vertical penetration

An interesting way to view the results of the three-dimensional model is in terms of horizontal averages

as in Fig. 12. It is readily apparent from this figure that the model without wintertime convection is not carrying tracer down into the ocean as efficiently as the data indicates it should. The addition of wintertime convection improves the simulation dramatically, particularly in the first three levels of the model. The tritium concentrations are near the error limit of the data at most levels, with the conspicuous exception of level 5, at 451 m, which will be discussed below.

A comparison of horizontal averages obscures the structural differences in the fields which have been discussed above. Another useful way of comparing the tritium fields that takes the structure of the fields into consideration, is to calculate the variance at each level. This is done by taking the area-weighted mean of the square of the difference between model and data, divided by the error estimate for the mapped data at each  $1^\circ$  grid point. The model results are first smoothed with the same smoothing function used in producing the data maps. The results are shown in Fig. 13. The model is fairly close to the 96% confidence limits of 2 at all levels except at 451 m. Also shown in Fig. 13 is the variance for the same model but without wintertime convection. As would be expected, the variance of the model without wintertime convection is far greater than that with wintertime convection.

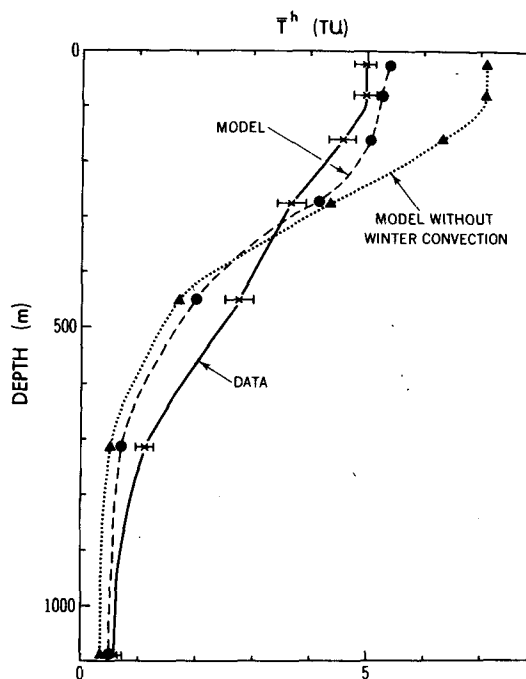


FIG. 12.  $\bar{T}^h$  at the end of 1972 as a function of depth for the model with wintertime convection described in the text, and for an identical model without wintertime convection.

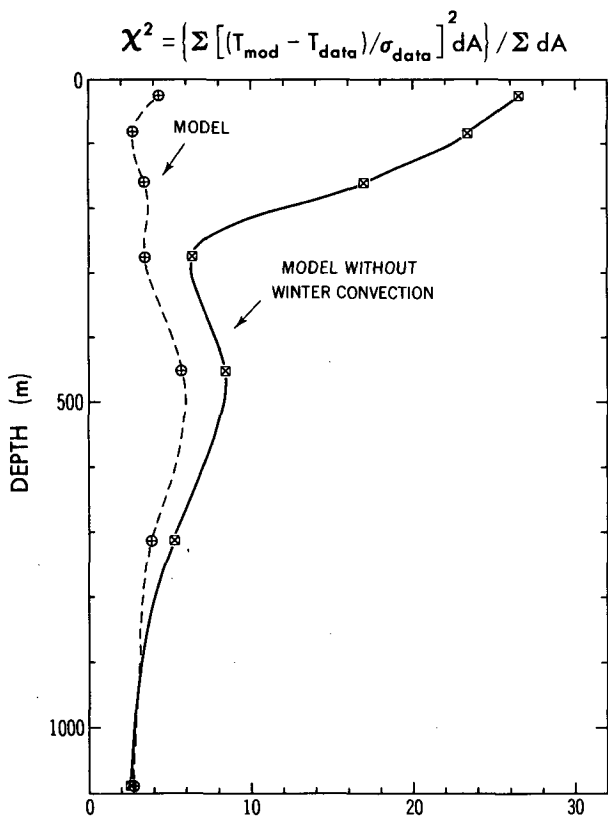


FIG. 13. Variance of the model described in the text and for the same model without convection. The data and error used in calculating the variance are described by Sarmiento *et al.* (1982b). The 96% confidence limit of the variance is 2. This is for 17 degrees of freedom which remain after smoothing of the data.

It is interesting to ask what the relative importance of advection, convection and mixing (due to the model  $A_{TV} = 0.5 \text{ cm}^2 \text{ s}^{-1}$ ) are in driving tracer downward in the model. One way to do this is to use an approach similar to that adopted by Mahlman (1975) in a study of atmospheric models, by calculating the vertical diffusivity  $K$  that satisfies the equation

$$\overline{\text{Flux}}^h = -K \frac{\partial \bar{T}^h}{\partial z}, \quad (8)$$

where the horizontal average is defined as

$$\overline{(\quad)}^h = \frac{\iint (\quad)_{\phi, \lambda} d\phi d\lambda}{\text{Area}_{z=0}}. \quad (9)$$

$\text{Area}_{z=0}$  is the area at the surface ( $z = 0$ ). Eq. (8) can be used to define a  $K_{\text{advective}}$ ,  $K_{\text{convective}}$ ,  $K_{\text{mixing}}$  and  $K_{\text{total}} = K_{\text{adv}} + K_{\text{conv}} + K_{\text{mix}}$  by dividing the flux into appropriate components. The calculations shown here

are for a given time step, i.e., there is no time averaging of the flux and tritium concentration.  $K_{\text{mix}}$  will only equal  $A_{TV}$  ( $0.5 \text{ cm}^2 \text{ s}^{-1}$ ) if  $(\partial T / \partial z)^h = \partial \bar{T}^h / \partial z$ . This is not always the case because of the sloping sides of the model ocean.  $K_{\text{mix}}$  varies between 0.4 and  $0.64 \text{ cm}^2 \text{ s}^{-1}$  in the upper 713 m. At most depths and for most times  $K_{\text{mix}}$  is very close to  $0.5 \text{ cm}^2 \text{ s}^{-1}$ .

$K_{\text{adv}}$  and  $K_{\text{conv}}$  are shown in Fig. 14 along with  $\bar{T}^h$  as a function of time. The diffusivities shown are those between each level from 1 to 6 (see Table 1 for depths of levels). It is clear from Fig. 14 that downward advection and convection completely overshadow the model mixing. The effect of convection is much greater than that of advection at most levels prior to 1966, but after this, the advection is somewhat larger than the convection. The importance of nonadvective processes in the tracer penetration is confirmed by the tritium box model study of Sarmiento (1983).

$K_{\text{adv}}$  starts out low at 50, 113 and 205 m, and increases with time. The reverse is true at 344 and 557 m.  $K_{\text{adv}}$  depends on the correlation between  $T$  and  $w$ . A high negative correlation corresponds to a large  $T$  where there is downwelling and a small  $T$  where there is upwelling. The tritium input is not correlated with  $w$  so  $K_{\text{adv}}$  starts out somewhat small. The circulation will tend to increase the negative correlation with time, up to a certain point, by decreasing the tritium in upwelling areas where tritium-free waters are brought up, and concentrating the tritium toward the downwelling areas. This is what happens at 50, 113 and 205 m. When sufficient time elapses, the upwelling waters will themselves have tritium (the isopycnal surfaces fill up with tritium) and  $K_{\text{adv}}$  will begin to drop again, as at 50 m after 1969 and at 113 m after  $\sim 1970$ .

At and below 205 m, the first tritium to arrive will have a large negative correlation with  $w$  because much of it comes down by advection;  $K_{\text{adv}}$  is thus very large when tracer is entering the ocean.  $K_{\text{adv}}$  begins to drop almost immediately (long before the isopycnal surfaces can fill up with tritium, as on shallower surfaces) because the vertical and horizontal mixing smooth the  $T$  field, slowly destroying the negative correlation between  $w$  and tritium concentration.

Because of the way  $K_{\text{adv}}$  depends on the negative correlation between  $T$  and  $w$ , one finds that an increase in the horizontal diffusion coefficient in the model, which helps to destroy this correlation, decreases  $K_{\text{adv}}$ . The overall penetration in a tracer simulation without convection thus decreases with increasing horizontal mixing.

$K_{\text{conv}}$  depends on a process which acts to smooth  $T$  out vertically over a specified depth range.  $K_{\text{conv}}$  is large during periods when the tracer is entering the surface of the ocean, but decreases rapidly when the tracer no longer is entering the ocean. At later times,

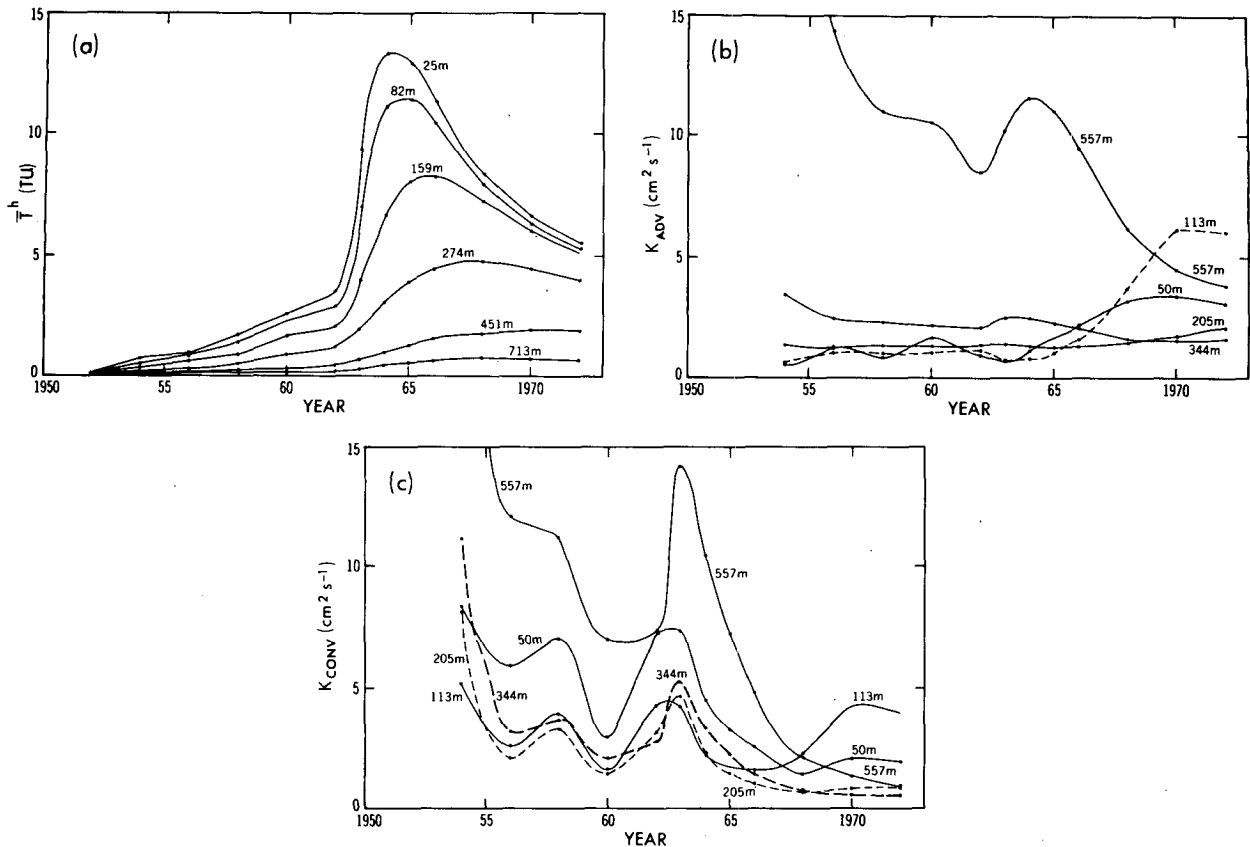


FIG. 14. (a)  $T^h$  as a function of time for various depths, (b)  $K_{adv}$  as a function of time and (c)  $K_{conv}$  as a function of time. Solid and dashed lines are used only to help separate lines that overlap substantially.

convection only leads to downward tracer penetration when horizontal advection and mixing feed in tracer laterally. The effect of a change in horizontal mixing in the model would depend on the concentration gradients between regions of deep convection and regions of shallow or no convection. In the model an increase in horizontal mixing feeds tracer *into* the convective regions and thus increases  $K_{conv}$ .

By 1972,  $K_{adv}$  at all levels shown in Fig. 14 except 113 m is trending toward a value of  $\sim 2.5 \text{ cm}^2 \text{ s}^{-1}$ ; and  $K_{conv}$ , also except at 113 m, is trending toward a value of  $\sim 1.0 \text{ cm}^2 \text{ s}^{-1}$ . The  $K$ 's at 113 m are anomalous because the vertical gradient in  $T^h$  (Fig. 14a) between 82 and 159 m is quite small. This is due primarily to the large penetration of tritium to 159 m in the Subtropical Underwater south of  $30^\circ\text{N}$ . The advection and convection are active primarily in regions to the north of this for which the  $\partial T^h / \partial z$  as calculated at 113 m is not representative.

Finally, a comparison of the model with the data is made on the basis of mean penetration depths  $z_*$ , calculated by taking the volume integral of tritium and dividing it by the area integral of tritium concentration at 25 m. The results are shown in Table 2. The model

$z_*$  is very close to the data  $z_*$ . More interesting, perhaps, is the low  $z_*$  obtained using the model described in this paper with the same total input, but smoothed so that it is no longer biased toward the high-latitude areas where the greatest vertical penetration occurs.

Broecker *et al.* (1979) have used calculations of penetration depths from tritium data to calibrate one-dimensional fossil fuel  $\text{CO}_2$  uptake models.  $\text{CO}_2$  is similar to the smoothed tritium input experiment, in that its input is relatively independent of latitude. Broecker *et al.* attempt to normalize out the high-latitude bias of the tritium input by calculating  $z_*$  locally and then averaging it horizontally. The model results give a penetration depth of 500 m using the

TABLE 2. Penetration depths calculated from the data and two versions of the model;  $z_*$  is defined in the text.

|                           | $z_*$<br>(m) |
|---------------------------|--------------|
| Data                      | 592          |
| Model                     | 543          |
| Model with smoothed input | 395          |

Broecker *et al.* technique. This is less than the 543 m penetration depth calculated by the technique described in the preceding paragraph, but still almost 27% higher than the 395 m penetration depth for the smoothed input function. These results suggest that great care must be exercised in applying the  $z_*$ 's obtained from tritium to tracers that have different boundary conditions.

#### 4. Discussion

This discussion will focus on the major problems of the low tritium concentrations within approximately the subtropical gyre at level 5 (451 m), and the loss of tracer from the gyre primarily to higher latitudes. These two problems are linked in that it is precisely at level 5 and below that the deficits in the subtropical gyre occur.

Sarmiento *et al.* (1982a) speculate that the entry of tritium into the subtropical gyre main thermocline occurs primarily in the wintertime along isopycnals by advection from the northeast and by cross-Gulf Stream/North Atlantic Current eddy transport in the northwest. The tritium entering from the northwest would get caught in the intense recirculation region that exists north of Bermuda.

There are several aspects of these processes which the model may not be simulating properly. The wintertime convection carrying tracer down to where it would get caught up in the gyre circulation on level 5 may not be deep enough. There is a great deal of variability with time in this process (Jenkins, 1982), and it is possible that the parameterization of wintertime convection used in the model underestimates the convective overturning that occurred during the period of tritium entry.

Another aspect of the tritium simulation that may be problematic is the mixing parameterization. The mixing in this model is oriented vertically and horizontally, whereas indications are that it should be oriented along isopycnals with a smaller, but important component normal to the isopycnals. The primary areas where this would make a significant difference is where isopycnals slope sharply downward from the surface as in the vicinity of the Gulf Stream/North Atlantic Current. Isopycnal mixing would, in these regions, provide a more effective means of entry of the tracer into the thermocline (Redi, 1982).

Finally, the non-uniformity of the mesoscale eddy field in the oceans, demonstrated, for example, by Dantzler (1976), may play an important role in the tracer redistribution that is not properly represented in the tritium model. This may be the case especially in the northwestern part of the subtropical gyre where the eddy energy is most intense. The eddies provide a mechanism for tritium entry into the subtropical gyre thermocline along isopycnals from regions of

high tritium input along the continental margin to the north and northwest of the gyre. In the model's present form, the components of the Gulf Stream and North Atlantic Current contributing to the meridional overturning rapidly remove tritium from the northwestern part of the gyre to higher latitudes. If more of the tritium in this region were transported southward across the Stream where it would have a chance to get caught up in the gyre recirculation region, less of it would be lost to higher latitudes.

In this connection, it is worth pointing out that the free thermocline model, because it is not eddy resolving, does not develop the intense recirculation north of Bermuda that Holland (1978) has demonstrated is a consequence of the eddies. The combination of greater penetration of tracer into the gyre as discussed above, and increased gyre recirculation north of Bermuda might increase the southward gyre transport of tracer noted above and thus compensate the northward loss of tracer due to the meridional component of tracer transport.

Another aspect of the model simulation which is not supported by the data is the tritium maximum at the surface in the region of the Ekman convergence (Fig. 13). It is likely that a deeper penetration of tritium at higher latitudes, as discussed above, would decrease the high concentrations in this region simply by removing tritium from the high-latitude surface waters that are converging to it. The fact that the maximum is much greater in a tritium simulation that has no wintertime convection supports this interpretation.

The tritium input function used in the model is obtained indirectly from observations of tritium concentration in rainfall (Weiss *et al.*, 1979). The uncertainty arising from the limitations of the rainfall data set and the assumption made by Weiss *et al.* contribute to a corresponding error in the model simulation. It is difficult to estimate the importance of this effect. The distribution of tritium within the oceans is certainly sensitive to the input, as shown in a gross way by the experiment with a smoothed input discussed in connection with Table 2. The errors in the input are almost certainly not that great, however, and the failure of the tritium to penetrate adequately to level 5 most likely arises from a combination of various physical processes missing from, or misrepresented in, the model. The limitations of the input function may become more significant as the simulations improve, and new oceanic measurements are obtained to place stronger constraints on the observed tritium distribution.

#### 5. Conclusions

The simulation of tritium with a primitive equation ocean circulation model clearly demonstrates the

enormous value of a tracer such as tritium for model calibration. This is particularly the case for what one can learn about the mechanisms and time scales of ventilation of subsurface waters with respect to surface waters. Information about these ventilation processes is difficult to obtain from other tracers. A correct characterization of ventilation processes is essential if we are to develop a predictive capability of the oceanic role in the earth's climate and in the uptake of pollutants. The tritium distribution also carries important information about mechanisms and rates of horizontal spreading processes within the subtropical gyre and across the boundaries of the gyre.

The tritium simulation discussed in this paper is able to reproduce most of the major features observed in the data. The low equatorial concentrations, due partly to the low input and partly to the removal of tracer by upwelling and northward transport of low tritium waters, are properly simulated. These same processes give rise to the tritium "front" at  $\sim 15^\circ\text{N}$ . Several details of the front resulting from the advection field, such as the northward slope of the front with increasing depth, and the northeast-to-southwest trend of the front, are also reproduced in the model.

North of the front, the tritium maximum in the Subtropical Underwater is reproduced. The maximum is seen to be a consequence of the northward advection of low-tritium equatorial water at the surface above the southward moving high-tritium Underwater.

The most significant downward penetration of tracer occurs at higher latitudes and is dominated by convection and downwelling. The effect of the model mixing ( $0.5 \text{ cm}^2 \text{ s}^{-1}$ ) is negligible. The subtropical gyre circulation spreads the tracer within the gyre once it has penetrated from the surface. The high-latitude processes are particularly effective in driving tracer downward in the model because the input is concentrated in these regions. Thus, a model with a smoothed input has a mean penetration depth of only 395 m as compared with the 545 m penetration of the "real" input with its strong high-latitude bias (Fig. 9).

The relative importance of convection and advection in tritium penetration into the model ocean is sensitive to the time elapsed since the peak input, and to horizontal transport and mixing. Convection dominates near the time of maximum input, whereas advection dominates after the input has dropped. It is interesting to note that there is some tendency for the changes to compensate each other so that the  $K_{\text{total}}$  is less sensitive to elapsed time than its components. Strong horizontal mixing tends to increase convective penetration and decrease advective penetration. Given this complexity, and the sensitivity of the penetration to the spatial distribution of the input, one needs to exercise great care in using simplified models

of one tracer to make predictions of tracers with different input functions.

The most serious problem in the model occurs at level 5 (451 m), where tritium concentrations are far less than the data indicate they should be. The tritium that should be at this level is lost to higher latitudes by the meridional overturning component of the tracer transport.

It is probably safe to say that tritium simulation does not point toward any major problems with the horizontal circulation in the upper 1000 m of the model, except for the absence of the eddy-generated intense recirculation north of Bermuda (Holland, 1978). This is to be expected inasmuch as the circulation in the oceans is thought to be primarily geostrophic, and the model temperature and salinity fields are in reasonably good agreement with the observed fields. Rather, the indication is that the major problems lie in correctly defining the vertical processes and in parameterizing the effect of horizontal eddy processes. A number of things that can be done about these problems, such as orienting the mixing tensor along and perpendicular to isopycnals, improving the parameterization of wintertime convection and working with eddy-resolving models, are being worked on at the present time.

In this connection it needs to be pointed out that the data would be far more useful if the coverage in regions of tracer penetration, such as off North America and in the northeastern Atlantic, were improved.

The tritium data set is being improved greatly by the work of the Transient Tracers in the Oceans Project (TTO). Tritium has now been in the ocean for on the order of two decades, and will not be as sensitive to the shorter time scales relevant to the upper part of the thermocline. However, its daughter, He-3, should prove extremely valuable. The coverage of data in the regions of tracer penetration, such as off North America and in the northeastern Atlantic, will also be greatly improved by the TTO work.

*Acknowledgments.* The author wishes to thank Kirk Bryan for the strong support he has given to this effort from the very beginning. K. Bryan, J. Mahlman, S. Manabe, G. Philander and an anonymous reviewer made very helpful comments on the manuscript. M. Jackson saw the manuscript through several typings. P. Tunison did the figures and J. Callan did the typing. This work was supported by the Visiting Scientist Program of Princeton University/NOAA, Grant 04-7-022-44017, ARL/NOAA Grant NA80 RAC-00156 and NSF Grant OCE 81-10155.

#### REFERENCES

- Arakawa, A., 1966: Computational design for long-term numerical integration of the equations of fluid motion: Two-dimensional incompressible flow. *J. Comput. Phys.*, 1, 119-143.

- Arons, A. B., and H. Stommel, 1967: On the abyssal circulation of the world ocean. III. An advective lateral mixing model of the distribution of a tracer property in an ocean basin. *Deep-Sea Res.*, **14**, 441-457.
- Broecker, W. S., and H. G. Ostlund, 1979: Property distributions along the  $\sigma_\theta = 26.8$  isopycnal in the Atlantic Ocean. *J. Geophys. Res.*, **84**, 1145-1154.
- , T.-H. Peng and M. Stuiver, 1978: An estimate of the upwelling rate in the equatorial Atlantic based on the distribution of bomb radiocarbon. *J. Geophys. Res.*, **83**, 6179-6186.
- , T. Takahashi, H. J. Simpson and T.-H. Peng, 1979: Fate of fossil fuel carbon dioxide and the global carbon budget. *Science*, **206**, 409-418.
- Bryan, K., 1969: A numerical method for studying the world ocean. *J. Comput. Phys.*, **1**, 347-376.
- Cox, M., 1983: A numerical model of the ventilated thermocline. *Ocean Modelling* (Unpublished manuscript).
- Dantzer, H. L., Jr., 1976: Geographic variations in the intensity of the North Atlantic and North Pacific Oceans eddy fields. *Deep-Sea Res.*, **23**, 783-794.
- Defant, A., 1936: *Schichtung und Zirkulation des Atlantischen Ozeans*. Meteor. Werk, Vol. 6, No. 1.
- Fiadeiro, M. E., 1982: Three-dimensional modeling of tracers in the deep Pacific Ocean. II. Radiocarbon and the circulation. *J. Mar. Res.*, **40**, 537-550.
- , and H. Craig, 1978: Three-dimensional modeling of tracers in the deep Pacific Ocean. I. Salinity and oxygen. *J. Mar. Res.*, **36**, 323-355.
- Holland, W. R., 1971: Ocean tracer distributions. *Tellus*, **23**, 371-392.
- , 1978: The role of mesoscale eddies in the general circulation of the ocean—numerical experiments using a wind-driven quasi-geostrophic model. *J. Phys. Oceanogr.*, **8**, 363-392.
- Hunt, B. G., and S. Manabe, 1968: Experiments with a stratospheric general circulation model. I. Radiative and dynamic aspects. *Mon. Wea. Rev.*, **96**, 477-539.
- Jenkins, W. J., 1980: Tritium and  $^3\text{He}$  in the Sargasso Sea. *J. Mar. Res.*, **38**, 533-569.
- , 1982: On the climate of the subtropical ocean gyre: decade timescale variations in water mass renewal in the Sargasso Sea. *J. Mar. Res.*, **40**, 265-290.
- Kuo, H. H., and G. Veronis, 1970: Distribution of tracers in the deep oceans of the world. *Deep-Sea Res.*, **17**, 29-46.
- , and —, 1973: The use of oxygen as a test for an abyssal circulation model. *Deep-Sea Res.*, **20**, 871-888.
- Levitus, S., 1982: *Climatological Atlas of the World Ocean*. NOAA Prof. Pap. No. 13, 173 pp.
- Mahlman, J. D., 1975: Some fundamental limitations of simplified-transport models as implied by results from a three-dimensional general-circulation/tracer model. *Proc. Fourth Conf. Climatic Impact Assessment Program*, T. M. Hard and A. J. Broderick, Eds., U.S. Dept. Transportation, 132-146.
- , D. G. Andrews, H. U. Dutsch, D. L. Hartman, T. Matsuno, R. J. Murgatroyd and J. F. Noxon, 1981: Transport of trace constituents in the stratosphere. *Handbook for MAP*, Vol. 3, *Middle Atmosphere Program*, C. F. Sechrist, Jr., Ed., SCOSTEP Secretariat, University of Illinois, 14-43.
- , H. Levy II and W. J. Moxim, 1980: Three-dimensional tracer structure and behavior as simulated in two ozone precursor experiments. *J. Atmos. Sci.*, **37**, 655-685.
- Mann, W. B., M. E. Unterwieser and B. M. Coursey, 1982: Comments on the NBS initiated water standards and their use. *Int. J. Appl. Radiat. Isotopes*, **33**, 383-386.
- Münnich, K. O., and W. Roether, 1967: Transfer of bomb  $^{14}\text{C}$  and tritium from the atmosphere to the ocean. Internal mixing of the ocean on the basis of tritium and  $^{14}\text{C}$  profiles. *Radioactive Dating and Method of Low-Level Counting*, Int. Atomic Energy Agency (IAEA), Vienna, 93-104.
- Östlund, H. G., M. O. Rinkel and C. G. H. Rooth, 1969: Tritium in the equatorial Atlantic current system. *J. Geophys. Res.*, **74**, 4535-4543.
- , R. Brescher and W. H. Peterson, 1974a: Ocean tritium profiles 1965-1972. Data Rep. No. 3, Rosenstiel School Mar. Atmos. Sci., University of Miami.
- , Dorsey, H. G. and C. G. H. Rooth, 1974b: GEOSECS North Atlantic radiocarbon and tritium results. *Earth Planet. Sci. Lett.*, **23**, 69-86.
- , — and R. Brescher, 1976: GEOSECS Atlantic radiocarbon and tritium results. Data Rep. No. 5, Rosenstiel School Mar. Atmos. Sci., University of Miami.
- , —, — and W. H. Peterson, 1977: Oceanic tritium profiles, NAGS Cruises 1972-73. Data Rep. No. 6, Rosenstiel School of Mar. Atmos. Sci., University of Miami.
- Redi, M. H., 1982: Oceanic isopycnal mixing by coordinate rotation. *J. Phys. Oceanogr.*, **12**, 1154-1158.
- Roether, W., and W. Weiss, 1978: A transatlantic tritium section near 40°N. "Meteor" *Forschungsbericht*, A., No. 20, 101-108.
- Rooth, C. G. H., and H. G. Östlund, 1972: Penetration of tritium into the Atlantic thermocline. *Deep-Sea Res.*, **19**, 481-492.
- Sarmiento, J. L., 1983: A tritium box model of the North Atlantic thermocline. *J. Phys. Oceanogr.*, **13**, 1269-1294.
- , and K. Bryan, 1982: An ocean transport model for the North Atlantic. *J. Geophys. Res.*, **87**, 394-408.
- , C. G. H. Rooth and W. Roether, 1982a: The North Atlantic tritium distribution in 1972. *J. Geophys. Res.*, **87**, 8047-8056.
- , J. Willebrand and S. Hellerman, 1982b: Objective analysis of tritium in the Atlantic Ocean during 1971-74. Tech. Rep. No. 1, Ocean Tracers Lab., Dept. Geol. Geophys. Sci., Princeton University, 19 pp.
- Semtner, A. J., and Y. Mintz, 1977: Numerical simulation of Gulf Stream and mid-ocean eddies. *J. Phys. Oceanogr.*, **1**, 208-230.
- Stommel, H., 1958: The abyssal circulation. *Deep-Sea Res.*, **5**, 80-82.
- Weiss, W., and W. Roether, 1980: The rates of tritium input to the world ocean. *Earth Planet. Sci. Lett.*, **49**, 435-446.
- , — and E. Dreisigacker, 1979: Tritium in the North Atlantic Ocean. *Behavior of Tritium in the Environment*, Int. Atomic Energy Agency (IAEA), Vienna, 315-336.